https://doi.org/10.5194/os-2020-69
Preprint. Discussion started: 21 July 2020

Ocean Science Discussions

High-resolution distributions of O_2/Ar on the northern slope of the South China Sea and estimates of net community production

Chuan Qin[1,2], Guiling Zhang[1,2,*], Wenjing Zheng[1], Yu Han[1,3], Sumei Liu[1,2]

1. Key Laboratory of Marine Chemistry Theory and Technology, Ministry of Education/Institute for Advanced Ocean Study, Ocean University of China, 238 Songling Road, 266100 Qingdao, P. R. China
2. Laboratory for Marine Ecology and Environmental Science, Qingdao National Laboratory for Marine Science and Technology, Qingdao 266237, P. R. China
3. Hainan Tropical Ocean University, Sanya 572022, P. R. China

* Correspondence to: Guiling Zhang (guilingzhang@ouc.edu.cn)

Abstract

Net community production (NCP) is a proxy of carbon export from the surface ocean and can be estimated based on O_2/Ar. In order to obtain the high-resolution distribution of NCP and improve our understanding of its regulating factors in the slope region of the Northern South China Sea (SCS), we conducted continuous measurements of dissolved O_2, Ar, and CO_2 by membrane inlet mass spectrometry during cruises in October 2014 and June 2015. An overall autotrophic condition was observed in the study region in both cruises with an average $\Delta(O_2/Ar)$ of 1.1 % ± 0.9 % in October 2014 and 2.7 % ± 2.8 % in June 2015. NCP was on average 11.5 ± 8.7 mmol C m^{-2} d^{-1} in October 2014 and 11.6 ± 12.7 mmol C m^{-2} d^{-1} in June 2015. Correlations between dissolved inorganic nitrogen (DIN), $\Delta(O_2/Ar)$, and NCP were observed in both cruises, indicating that NCP is subject to the nitrogen limitation in the study region. In June 2015, we observed a rapid response of the ecosystem to the episodic nutrient supply induced by eddies. Eddy-entrained shelf water injection, which supplied large amounts of terrigenous nitrogen to the study region, resulted in high productivity along a transect. In addition, upwelling brought large uncertainties to the estimation of NCP at the core region of the cold eddy (cyclone) in June 2015. The correlation between the volumetric NCP (NCP_{vol}) and the mixed layer depth (MLD) indicated that light availability may have also been a factor in influencing NCP in the SCS.

Keywords: O_2/Ar; Net community production; Nutrients; Eddy; Northern South China Sea

1. Introduction

The oceanic CO_2 uptake is partially regulated by the production and export process of biological organic carbon in the surface ocean. Net community production (NCP) corresponds to gross primary production (GPP) minus community respiration (CR) in the water (Lockwood et al., 2012) and is an important indicator of carbon export. Dissolved oxygen-to-argon ratio (O_2/Ar) has been developed as a proxy for NCP in a water mass based on the similar physical properties of O_2 and Ar (Craig and Hayward, 1987; Kaiser et al., 2005). Recently, the biological production in the oceans (i.e., Southern Ocean, North Pacific, Arctic Ocean) has been inferred using the O_2/Ar ratio to estimate NCP (Hamme et al., 2012; Lockwood et al., 2012; Ulfsbo et al., 2014; Shadwick et al., 2015; Izett et al., 2018). Although high-resolution distributions of O_2/Ar and NCP have been reported for coastal Antarctica waters (Tortell et al., 2014; Eveleth et al., 2017), observations in coastal waters remain sparse (Manning et al., 2017; Tortell et al., 2012). Despite coastal waters (including shelves and estuaries) only account for 7 % of the global ocean surface area, they are known to contribute to 15–30 % of the total oceanic primary production (Bi et al., 2013; Cai et al., 2011). Therefore, coastal waters play an important role in marine carbon cycle and production, and can provide a considerable expansion for the global NCP data sets.

The South China Sea (SCS) is one of the largest marginal seas in the world with extremely complex ecological characteristics. River runoff from the Pearl and Mekong Rivers introduces large amounts of dissolved nutrients into the SCS (Ning et al., 2004). Due to the prevailing southwest (northeast) monsoon, the surface circulation in the SCS basin is an anticyclonic (cyclonic) gyre during summertime (wintertime) (Hu et al., 2000). Feng et al. (1999) categorized the surface water of the SCS into three regimes: shelf water, offshore water (the Kuroshio water), and the SCS water. The shelf water is mixed with fresh water from rivers or coastal currents and thus usually has low salinity (< 32) and low density. The salinity of the surface water in SCS mixed with the shelf water is usually lower than 33 (Uu and Brankart, 1997; Su and Yuan, 2005; Cheng et al., 2014). The Northern Pacific is considered the source of both offshore water and

https://doi.org/10.5194/os-2020-69
Preprint. Discussion started: 21 July 2020

SCS water. Thus offshore water has similar hydrographic characteristics as the Northern Pacific water (high temperature and high salinity), but the SCS water has changed a lot because of the mixing with shelf water (Feng et al., 1999). The distributions of phytoplankton and primary productivity of the SCS show great temporal and spatial variation (Ning et al., 2004). Low chlorophyll-a (Chl a) and primary production are the significant characteristics of the SCS basin which is considered an oligotrophic region, and macronutrients (i.e. nitrogen and phosphorus) are the main limitations of phytoplankton growth and productivity (Ning et al., 2004; Lee Chen, 2005; Han et al., 2013). In contrast, the estuaries and the continental shelf in the SCS are generally characterized by high primary production (Lee Chen, 2005).

Little research has been conducted on NCP in the SCS to date. Chou et al. (2006) estimated NCP in the northern SCS to be 4.47 mmol C m^{-2} d^{-1} based on the dissolved inorganic carbon (DIC) concentration in the mixed layer at the South East Asia Time-Series Station (SEATS) from 2002 to 2004. Wang et al. (2014) used GPP and community respiration data from an incubation experiment to calculate NCP in the northern SCS and obtained a range from −179.0 to 377.6 mmol O_2 m^{-2} d^{-1}. A few studies were conducted on particulate organic carbon (POC) flux in the SCS. Chen et al. (1998) collected particles in the SCS using sediment traps at depths from 1000 m to 3770 m and reported that POC export from the surface water was 10.32–12.93 g C m^{-2} a^{-1} which was strongly influenced by the monsoon. Chen et al. (2008) quantified POC export rates in the northern SCS using the $^{234}Th/^{238}U$ disequilibrium method and derived a range of POC flux of 5.3 to 26.6 mmol C m^{-2} d^{-1} with insignificant seasonality. Cai et al. (2015) estimated the mean POC export fluxes from the euphotic zone to be 24.3, 18.3, and 6.3 mmol C m^{-2} d^{-1}, respectively for the coastal, shelf, and basin regimes based on ^{234}Th and POC data collected during 4 oceanographic surveys. However, these studies in the SCS were constrained by methodological factors attributed to discrete sampling and cannot reveal the rapid productivity response to highly dynamic environmental fluctuations of coastal systems. In this paper, we present high-resolution NCP estimates in the northern slope region of the South China Sea based on continuous shipboard dissolved O_2/Ar measurements. We discuss the regulating factors of NCP and $\Delta(O_2/Ar)$ based on ancillary measurements of other hydrographic parameters. We also report on the rapid response of the ecosystem to the episodic nutrient supply induced by eddies.

2. Methods

2.1 Continuous underway sampling and measurement

Continuous measurements of dissolved O_2, Ar, and CO_2 were obtained using membrane inlet mass spectrometry (MIMS) (HPR 40, Hiden Analytical, UK) onboard the *RV* 'Nanfeng' during two cruises in the northern slope region of the South China Sea (Figures 1a, b) from 13 to 23 October 2014 and from 13 to 29 June 2015. In addition, a cyclonic-anticyclonic eddy pair was observed in June 2015 (Figure 1c) and resulted in dramatic influences on the study region.

We developed a continuous shipboard measurement system of dissolved gases following the method described by Guéguen and Tortell (2008). Surface seawater was collected continuously using the ship's underway intake system (~5 m depth) and was divided into different lines for various underway scientific measurements. Seawater from the first line passed through a chamber at a flowrate of 2–3 L min^{-1} to remove macroscopic bubbles and to avoid pressure bursts. A flow of ~220 mL min^{-1} was continuously pumped from the chamber using a Masterflex Peristaltic Pump equipped with L/S® multichannel cartridge pump heads (Cole Parmer). In order to minimize the O_2/Ar fluctuations due to temperature effects and water vapor pressure variations, the water samples flowed through a stainless steel coil (~6 m) with 0.6 mm wall thickness immersed in a water bath (Shanghai Bilon Instrument Co. Ltd, China) to achieve a constant temperature (~2 ºC below the sea surface temperature), which avoided temperature-induced supersaturation and subsequent bubble formation. Then the water samples were introduced into a cuvette with a silicone membrane mounted on the inside. The analyte gases were monitored by a Faraday cup detector in the vacuum chamber after diffusion through the silicone membrane, and the signal intensities at the relevant mass to charge (m/z) ratios (32, 40 and 44 for O_2, Ar and CO_2, respectively) were

https://doi.org/10.5194/os-2020-69
Preprint. Discussion started: 21 July 2020

Ocean Science Discussions

recorded by MASsoft. Based on the continuous measurement of 50 L air-equilibrated seawater, the long-term signal stability (measured as the coefficient of variation) over 12 h was 1.57 %, 3.75 % and 2.21 % for O_2, Ar and CO_2, respectively. Seawater from the second line passed through a flow chamber, where an RBR Maestro (RBR, Canada) was installed to continuously record temperature, salinity, dissolved oxygen (DO), and Chl a. A third line was used to drain the excess seawater. Underway pipelines were flushed with freshwater or bleach every day, to avoid possible in-lines biofouling. The data from the underway transects were exported to spreadsheets and compiled into 5 min averages, and the comparisons of the gas data with other hydrographic variables were based on the UTC time recorded for each measurement.

The O_2/Ar ratio measurements were calibrated with air-equilibrated seawater samples at about 6–8 h intervals to monitor instrument drift and calculate $\Delta(O_2/Ar)$. These air-equilibrated seawater samples were prefiltered (0.22 μm) and bubbled with ambient air for at least 24 h to reach equilibrium at sea surface temperature (Guéguen and Tortell, 2008). For calibration, 800 mL of air-equilibrated seawater sample was transferred into glass bottles and immediately drawn into the cuvette, where the first 200 mL of the sample was used to flush the cuvette and pipelines. After 3 min recirculation of the sample, the average signal intensity was obtained to calculate O_2/Ar. During the course of measurements, flow rate and the temperature of water bath were both kept the same as the underway measurements. The precision of MIMS-measured O_2/Ar was 0.22 %, based on analyses of 20 duplicate samples in the laboratory test, which is comparable to previous studies and sufficient to detect biologically driven gas fluctuations in seawater (Tortell, 2005).

The instrumental CO_2 ion current was calibrated at about 12–24 h intervals using equilibrated seawater standards as per Guéguen and Tortell (2008) during the survey in June 2015. Prefiltered seawater (0.22 μm) was gently bubbled with dry CO_2 standards (200, 400, and 800 ppm, provided by the Chinese National Institute of Metrology) at in situ temperature. After 2 days of equilibrium, these standards were analyzed by MIMS following the same procedure for measuring air-equilibrated seawater samples to obtain a calibration curve between CO_2 signal intensity and mole fraction. The reproducibility

https://doi.org/10.5194/os-2020-69
Preprint. Discussion started: 21 July 2020

of these measurements was better than 5 % within 15 days. Then we used the empirical equations reported by Takahashi et al. (2009) to convert the CO_2 mole fraction derived from the calibration curve to the in situ partial pressure of CO_2 ($p$$CO_2$).

Chlorophyll-a (Chl a) data from the RBR sensor were linear calibrated against extracted Chl a measurements of discrete seawater samples taken from the same seawater outlet as for MIMS measurements. Samples were filtered through polycarbonate filters (0.22 μm). The filter membranes were then packed with pre-sterilized aluminum foil and stored in a freezer (−20 °C) until extraction by acetone and analysis using a fluorimetric method (F-4500, HITACHI, Japan) described by Parsons (1984). The mean residual of this calibration was 0.00 ± 0.07.

2.2 Estimation of NCP based on O_2/Ar measurements

NCP in the mixed layer was estimated by the O_2/Ar mass balance from continuous measurements. Due to similar physical properties of O_2 and Ar, $\Delta(O_2/Ar)$ is used as a proxy of the biological O_2 supersaturation and is defined as (Craig and Hayward, 1987):

$$\Delta(O_2/Ar) = \frac{([O_2]/[Ar])}{([O_2]/[Ar])_{eq}} - 1$$

where $[O_2]/[Ar]$ is the measured dissolved O_2/Ar ratio of the mixed layer and $([O_2]/[Ar])_{eq}$ is the measured dissolved O_2/Ar ratio of the air-equilibrated seawater samples. $\Delta(O_2/Ar)$ is the percent deviation of the measured O_2/Ar ratio from the equilibrium. Assuming a steady state and negligible physical supply, NCP is the air–sea biological O_2 flux and can be estimated as (Reuer et al., 2007):

$$NCP\ (mmol\ C\ m^{-2}\ d^{-1}) \approx k_{O_2} \cdot [O_2]_{sat} \cdot \Delta(O_2/Ar) \cdot r_{C:O_2} \cdot \rho$$

where k_{O_2} is the weighted gas transfer velocity of O_2 (m d^{-1}); $[O_2]_{sat}$ denotes the saturation concentration of dissolved O_2 (μmol kg^{-1}) in the mixed layer, which is calculated based on temperature and salinity (Weiss, 1970); $r_{C:O_2}$ is the photosynthetic quotient of C and O_2 and was reported as 1:1.38 in the SCS (Jiang et al., 2011); ρ is seawater density in units of kg L^{-1} (Millero and Poisson, 1981). We estimated k_{O_2} using the European Centre for Medium-Range Weather Forecasts (ECWMF) wind-

https://doi.org/10.5194/os-2020-69
Preprint. Discussion started: 21 July 2020

speed reanalysis data product with a 0.25° × 0.25° grid (https://www.ecmwf.int), the parameterization by Wanninkhof (1992), and the gas exchange weighting algorithm by Teeter et al. (2018). However, Teeter et al., (2018) pointed out that O_2/Ar method does not strongly rely on the steady state assumption. When this assumption is violated, our estimate does not represent the actual daily NCP but rather an excellent estimate of NCP weighted over the past month and along the path of the water parcel during that period

2.3 Ancillary measurements

Surface water samples for the nutrient analysis were collected from Niskin bottles mounted on the CTD, where the samples were filtered through acid-cleaned acetate cellulose filters (pore size: 0.4 μm). The filtrates were poisoned by $HgCl_2$ and stored in the dark at 4 °C. In the laboratory, the nutrients were determined photometrically by an auto-analyzer (QuAAtro, SEAL Analytical, Germany) with a precision better than 3 %. The mixed layer depths (MLDs) were defined by the $\Delta\sigma_t$ = 0.125 kg m^{-3} criterion (Monterey and Levitus, 1997), and the euphotic depths (z_{eu}) were calculated by the model-derived formula based on the surface Chl a concentration (Zheng et al., 2018). The MLDs and the euphotic depths were calculated at the stations where the vertical CTD casts were made. The MLDs for underway data between CTD stations was calculated using linear interpolation based on the distance between the underway points and nearest CTD stations. We matched the underway data to each CTD location using a combination of latitude/longitude threshold (latitude/longitude of CTD station ± 0.05°) and time threshold (end/start of stationary time ± 1 h), then took the averages of these underway data for further analysis with discrete nutrient concentrations and MLDs.

3. Results and Discussion

3.1 Distributions of hydrographic parameters and gases

The distributions of temperature, salinity, Chl a, and $\Delta(O_2/Ar)$ during the autumn cruise (October 2014) are shown in Figure 2. Sea surface temperature (SST) ranged from 26.96 °C to 28.53 °C with an average of 27.82 ± 0.33 °C. Sea surface salinity (SSS) ranged from 33.28 to 34.11 with the low values occurring in the southeast of the region. Chl a concentration was in an average of 0.18 ± 0.13 μg L^{-1}, which was comparable to the 11-year mean value (~ 0.2 mg m^{-3}) in the same region in October reported by Liu et al. (2014). $\Delta(O_2/Ar)$ values were in the range of −2.9–4.9 % (avg. 1.1 % ± 0.9 %) and most areas were slightly oversaturated (Figure 2d).

In June 2015, SST ranged from 29.28 °C to 32.24 °C and was in an average of 30.88 ± 0.59 °C. Transect 3 was significantly characterized by low salinity (Figure 3b). He et al (2016) reported that this phenomenon was influenced by the eddy-entrained Pearl River plume injected into the SCS. Under the influence of this plume water, Chl a values higher than 0.30 μg L^{-1} were observed along Transect 3 (Figure 3c). In contrast, Chl a was in the range of 0.09–0.18 μg L^{-1} along Transect 1 and 2. It was obvious that DO was much higher in the east side than the west side in the study region (Figure 3d). Most of the $\Delta(O_2/Ar)$ values were positive in the region (avg. 2.7 % ± 2.8 %), whereas the negative values were concentrated along Transect 4 (Figure 3f). pCO$_2$ exhibited a high degree of spatial and temporal variability and the high values mostly occurred on the west side of the study region (Figure 3e). Resulting from the considerable low pCO$_2$ in Transect 3 (avg. 222 ± 33 μatm), the average pCO$_2$ (323 ± 93 μatm) in this region was lower than those reported previously, i.e., 350–370 μatm by Zhai et al (2009) and 340–350 μatm by Rehder and Sues (2001). Due to the influence of the plume water, Transect 3 showed high $\Delta(O_2/Ar)$ and low pCO$_2$, which was presumably indicative of a strong biological CO_2 sink.

3.2 NCP in autumn and summer

In October 2014, NCP in the northern slope of the SCS ranged from −29.2 to 42.7 mmol C m^{-2} d^{-1} (avg. 11.5 ± 8.7 mmol C m^{-2} d^{-1}) and most of the region was net autotrophic (Figure 4a). The estimated NCP based on the O_2/Ar values measured in this cruise is about 34 % of the net primary production rates measured by ^{14}C bottle incubation (34.3 mmol C m^{-2} d^{-1} on average, Sun X., personal communication), which was in agreement with previous research (Quay et al., 2010).

The average NCP in the study region was 11.6 ± 12.7 mmol C m^{-2} d^{-1} with a range of

https://doi.org/10.5194/os-2020-69
Preprint. Discussion started: 21 July 2020

−27.6–61.4 mmol C m^{-2} d^{-1} in June 2015. A high NCP level was observed along Transect 3 (Figure 4b). Eddy-entrained shelf water brought a large amount of terrigenous nutrients from the shelf to the slope region along Transect 3 (He et al., 2016). The average NO_3^- and NO_2^- concentrations in the surface water of Transect 3 were 2.31 ± 0.70 μmol L^{-1} and 0.04 ± 0.01 μmol L^{-1} respectively (Figure S2a, b); both values were much higher than those found in the other three transects (NO_3^- was in a range of < 0.03–0.69 μmol L^{-1} and NO_2^- was mostly below the detection limit). Li et al. (2018) reported that the entire Transect 3 and the south end of Transect 4 were dominated by shelf water at the surface and we estimated NCP over these regions (also including the north end of Transect 4) where salinity lower than 33.0 as 23.8 ± 10.7 mmol C m^{-2} d^{-1} on average. We also observed a warm eddy (anti-cyclone) covering most stations in Transects 1 and 2 (Figure 1b, c) during our survey in June 2015 (Chen et al., 2016). Anti-cyclonic eddies can cause downwelling, deepening of the thermocline, and blocking of the supply of nutrients from the deeper water (Ning et al., 2008; Shi et al., 2014). Consequently, a warm eddy is expected to result in an oligotrophic condition in the surface water associated with low Chl a concentrations and low production (Ning et al., 2004). As a result, in the summer of 2015, the observed NO_2^-, NO_3^-, and PO_4^{3-} concentrations were almost below the detection limit in Transects 1 and 2 (Figure S2a, b, d). The NCP in Transect 1 and 2 (including the underway data along the cruise track between Transect 1 and 2) was at a very low level (avg. 2.8 ± 2.7 mmol C m^{-2} d^{-1}). Chou et al. (2006) estimated that NCP was on average 4.47 mmol C m^{-2} d^{-1} during the summer from 2002 to 2004 based on DIC budget in the SCS, indicating a lower value than our result in the summer of 2015. However, NCP estimations based on discrete sampling (or on-deck incubation) suffer from poor coverage and do not allow for revealing rapid changes in shelf systems. In contrast, continuous measurements of O_2/Ar allow us to capture rapid variations in NCP along Transect 3 and resolve short-term productivity responses to environmental fluctuations.

3.3 Distribution of various parameters along representative transects

We chose Transect 5 (Figure 1a) measured in October 2014 and Transect 4 (Figure 1b)

https://doi.org/10.5194/os-2020-69
Preprint. Discussion started: 21 July 2020

Ocean Science
Discussions
Open Access
EGU

measured in June 2015 to show the distribution of various parameters.

The distribution of Chl a, $\Delta(O_2/Ar)$, and NCP showed similar trend along Transect 5 in October 2014 (Figure 5). A spike of Chl a occurred between 115.6°E and 115.7°E and was coincident with the peaks of $\Delta(O_2/Ar)$ and NCP (Figure 5b, c). The highest surface concentration of NH_4^+ (0.35 μmol L^{-1}) was also observed between 115.6°E and 115.7°E in this transect and was predominantly higher than the concentrations (0.07–0.17 μmol L^{-1}) in the other regions of this cruise (Figure 5c, S1b). Because no obduction processes (i.e., upwelling, entrainment, and diapycnal mixing) were reported in this region, the most likely source of this abundant NH_4^+ was in situ regeneration. The excretion of zooplankton and the bacterial decomposition of organic matter were considered to be the main mechanisms for the release of NH_4^+ into the surface water (La Roche, 1983; Clark et al., 2008). Ammonium is an important nitrogen source of phytoplankton growth, which can be quickly utilized by phytoplankton, and contributes to primary production (Dugdale and Goering, 1967; Tamminen, 1982). Though we only got nutrient data at two CTD stations in this transect, the result partly indicated that higher ammonium could result in higher $\Delta(O_2/Ar)$ and NCP.

A similar distribution pattern of Chl a, NCP, and $\Delta(O_2/Ar)$ was observed along Transect 4 in June 2015, whereas pCO_2 showed the opposite trend for these three parameters (Figure 6b, c). Low salinity (lower than 33) existed at both southern and northern end of this transect (Figure 6a). The concentration of dissolved inorganic nitrogen (DIN, NO_3^- + NO_2^- + NH_4^+) in the surface water was 0.81 μmol L^{-1} (0.27 μmol L^{-1}) at the southern (northern) end and was higher than the concentrations in other stations of this transect (Figure 6c). These results indicate that shelf water is imported at the northern and southern end of this transect, along with higher levels of Chl a and NCP (Figure 6c). A sharp drop in the temperature and an increase in salinity occurred from 19.6°N to 19.8°N (Figure 6a), manifesting an upwelling over this area together with a dramatic spike in pCO_2 and an associated decrease in $\Delta(O_2/Ar)$ (Nemcek et al., 2008) (Figure 6b). A localized cold eddy was considered to be the cause of this upwelling, and most regions of Transect 4 were dominated by upwelling and showed negative sea level height anomaly (Chen et al., 2016; He et al., 2016).

https://doi.org/10.5194/os-2020-69
Preprint. Discussion started: 21 July 2020

Ocean Science
Discussions
Open Access

Upwelled deep waters are characteristic of low O_2/Ar signatures and are subject to oxygen loss due to respiration (Nemcek et al., 2008), resulting in the undersaturation of $\Delta(O_2/Ar)$ at the surface. Vertical mixing is considered the largest source of error in O_2/Ar-based NCP estimates because the negative $\Delta(O_2/Ar)$ resulting from upwelling may cause an underestimation of NCP in the surface water (Cassar et al., 2014). Cassar et al. (2014) presented an N_2O-based correction method of O_2/Ar and NCP for vertical mixing. Although this method has been successfully adopted by Izett et al. (2018) in the Subarctic Northeast Pacific, it is not suitable for our study region. This is because it is basically applicable in areas where the depths of euphotic zone and mixed layer are similar, and this method is not suitable for oligotrophic regions (Cassar et al., 2014). The SCS is recognized as an oligotrophic region and the depth of the euphotic zone can be 2–7 times that of the mixed layer in our study region in summer. In addition, in the region (e.g. the SCS) where subsurface oxygen maximum exists, upwelled water theoretically has a chance to cause an overestimation on surface $\Delta(O_2/Ar)$ and NCP. If we roughly neglect the regions with these underestimated (overestimated) NCP values caused by upwelling (neglecting the regions with salinity higher than 33.5 in Transect 4), the average NCP in June 2015 can slightly raise to 12.5 ± 12.5 mmol C m^{-2} d^{-1}. If we also remove the influence of shelf water injection (neglecting the regions with salinity lower than 33), the average NCP can sharply decrease to 4.9 ± 6.2 mmol C m^{-2} d^{-1}, which was similar to the results of 4.47 mmol C m^{-2} d^{-1} and 0.17 mol C m^{-2} $month^{-1}$ (~5.67 mmol C m^{-2} d^{-1}) reported in previous researches in the SCS (Chou et al., 2006; Huang et al., 2018).

3.4 Factors influencing $\Delta(O_2/Ar)$ and NCP in the SCS

The SCS is an oligotrophic region with low biomass and primary production (Lee Chen, 2005; Ning et al., 2004). Previous research has shown that the nutrient, especially nitrogen and phosphorus, is the most important factor controlling and limiting the phytoplankton biomass and primary production in the SCS (Ning et al., 2004; Lee Chen, 2005; Lee Chen and Chen, 2006; Han et al., 2013). After neglecting the regions (including two CTD stations) influenced by upwelling in June 2015, we performed a

https://doi.org/10.5194/os-2020-69
Preprint. Discussion started: 21 July 2020

principal component analysis (PCA) to determine the dominant factors influencing NCP in both cruises. In October 2014, DIN (0.741), $\Delta(O_2/Ar)$ (0.858), and NCP (0.979) were significantly loaded on Factor 1, indicating a potential relationship among these three variables (Figure 7a, Table S1b). The correlation coefficient between DIN and NCP was 0.706 (p < 0.01, Table S1a), which was significantly higher than the coefficient between NCP and the other variables, except for $\Delta(O_2/Ar)$ and temperature; this indicated that DIN was an important factor influencing NCP in this cruise. Another two nutrients – dissolved silicate (DSi, SiO_3^{2-}) and dissolved inorganic phosphorus (DIP, PO_4^{3-}) – had no correlations (p > 0.05) with NCP (Table S1a). In June 2015, Factor 1 showed a strong loading by DIN (0.876), Chl a (0.950), DO (0.927), $\Delta(O_2/Ar)$ (0.902), and NCP (0.909), whereas salinity (−0.936) and pCO$_2$ (−0.908) were negatively loaded on Factor 1 (Figure 7b, Table S2b). The injection of low salinity shelf water appeared to have a strong effect on the study region because significant negative correlations were observed between salinity and DIN, Chl a, $\Delta(O_2/Ar)$, and NCP (Table S2a). DIN had strong correlations with NCP, $\Delta(O_2/Ar)$, and Chl a (the correlation coefficients were 0.747, 0.910, and 0.754 respectively, Table S2a), indicating that DIN was the dominant factor controlling the growth of phytoplankton and primary production in this cruise. DSi (0.582) and DIP (−0.601) were both moderately loaded on Factor 2 (Figure 7b, Table S2b) and had no correlations with NCP (p > 0.05, Table S2a). These results suggested the key role of nitrogen in regulating $\Delta(O_2/Ar)$, NCP, and phytoplankton biomass in the SCS. The supply of nitrogen may stimulate the growth of phytoplankton in the SCS and nitrogen is an important participant in photosynthesis and a basic element that contributes to the increase in primary production (Dugdale and Goering, 1967; Lee Chen, 2005; Lee Chen and Chen, 2006; Han et al., 2013).

Coupled with biochemical variations, physical processes also play important roles in the slope region of the SCS by transporting abundant nutrient-rich shelf water into the SCS and bringing deep water to the surface by enhancing water mixing (Chen and Tang, 2012; Ning et al., 2004; Pan et al., 2012). The surface waters in the slope region of the northern SCS are primarily composed of waters originating from SCS water, Kuroshio water, and shelf water (Li et al., 2018). In the summer, the shelf water exists where the

https://doi.org/10.5194/os-2020-69
Preprint. Discussion started: 21 July 2020

potential density anomaly is lower than 20.5 kg m^{-3} (Li et al., 2018). In the fall, there is a weak offshore transport of the shelf water in the SCS and the salinity of the water mixed with the shelf water is usually lower than 33 (Fan et al., 1988; Uu and Brankart, 1997; Su and Yuan, 2005). In October 2014, the observed surface salinity was in a range of 33.28 to 34.11; thus the surface waters were mainly derived from mixing of the Kuroshio water and the SCS water. In the summer of 2015, a cyclonic-anticyclonic eddy pair was observed in the study region (Figure 1c). Low-salinity shelf water mixed with the intruding plume water from the Pearl River in the upper 50 m and was transported to the slope and basin along the intersection of the two eddies (Chen et al., 2016; He et al., 2016; Li et al., 2018). In both seasons, the surface waters in the study region were generally found to be nitrogen deficient, with nitrite at < 0.01–0.04 μmol L^{-1} (Figure S1a, S2b), nitrate at < 0.03–2.82 μmol L^{-1} (Figure S2a), and ammonium at 0.04–0.35 μmol L^{-1} (Figure S1b, S2c). The concentrations of nitrate and nitrite were below the detection limit at almost 80% of the sampling stations during both cruises. Due to the injection of shelf water with low salinity and abundant terrestrial nutrients, significant high concentrations of NO_3^- and NO_2^- were observed along Transect 3 in June 2015 (Figure S2a, b) where the shelf water was intruded by eddies (Chen et al., 2016; He et al., 2016). Such transport processes from the inner shelf to the slope region have a profound influence on nutrient dynamics and biological productions (He et al., 2016). The water that was influenced by shelf water with a potential density anomaly lower than 20.25 kg m^{-3} and salinity lower than 33.0 had high concentrations of DIN (Figure 8a). At the 6 stations (in the red circle of Figure 8a) that were intruded by shelf water and characterized with surface salinity lower than 33.0, we obtained an average surface DIN concentration of 1.82 ± 1.16 (0.27–3.01) μmol L^{-1}, which was significantly higher than the mean of 0.10 ± 0.03 (0.04–0.16) μmol L^{-1} at other stations (independent samples t-test, $p < 0.01$). In addition, a strong correlation between NCP (at the CTD stations without the influence of upwelling) and DIN was observed during the cruise of June 2015 (r = 0.747, $p < 0.01$), with higher NCP (avg. 15.4 ± 4.5 mmol C m^{-2} d^{-1}) occurred where shelf water intruded, consistent with the DIN concentration higher than 0.27 μmol L^{-1} (Figure 8b). At other stations without the influence of shelf water, the

https://doi.org/10.5194/os-2020-69
Preprint. Discussion started: 21 July 2020

average NCP was just 2.3 ± 1.7 mmol C m^{-2} d^{-1}. Compared to NCP, Δ(O_2/Ar) had a stronger correlation with DIN (r = 0.910, p < 0.01). The shelf water intrusion also caused a significant increase in Δ(O_2/Ar) (Figure 8c). These results furtherly suggest that the supply of DIN from shelf water can greatly stimulate the primary production in this region, resulting in the NCP increase of nearly 7 times compared to other regions.

The correlations between Δ(O_2/Ar), NCP and physical parameters (sea surface temperature and salinity) also support the influence of physical forcing on Δ(O_2/Ar) and NCP. In June 2015, we obtained strong negative correlations between Δ(O_2/Ar), NCP, and salinity (Figure 9f, h). Both Δ(O_2/Ar) and NCP significantly increased in the water with salinity lower than 33 (Figure 9f, h). Temperature had weak correlations with both Δ(O_2/Ar) and NCP (Figure 9e, g), and the negative Δ(O_2/Ar) and NCP values were concentrated in the water with temperatures below 30.5°C and salinity values over 33.5 (Figure 9e, f, g and h). This surface water was mostly observed along Transect 4 where vertical mixing caused by a cold eddy brought deep water to the surface. The undersaturated Δ(O_2/Ar) entrained by deep water caused the negative NCP estimates at the surface, resulting in a considerable underestimation of NCP. Unlike in June 2015, all the correlations were very weak or not statistically significant between Δ(O_2/Ar), NCP and temperature, salinity in October 2014 (Figure 9a, b, c and d). The Kuroshio water and the SCS water had similar hydrological characteristics and their mixing in October 2014 may not have resulted in significant changes in the hydrological characteristics of the surface water.

Light availability may also play a role in the primary production of the SCS (Lee Chen, 2005). The MLD is considered an important driver of light availability in the mixed layer (Cassar et al., 2011; Hahm et al., 2014). We used the volumetric NCP (NCP_{vol}; mmol C m^{-3} d^{-1}), which is the ratio of NCP to MLD to normalize NCP variation caused by a variable MLD (Hahm et al., 2014). To minimize the influence of physical processes and nutrient concentrations, we selected 9 stations (criterion: DIN < 0.36 μmol L^{-1}) with similar hydrographic and nutrient conditions in October 2014 and 6 stations (criterion: NCP < 2 mmol C m^{-2} d^{-1}) that were all under the influence of warm eddy in June 2015 (Figure 1c) during the respective cruise to analyze the influence of light

https://doi.org/10.5194/os-2020-69
Preprint. Discussion started: 21 July 2020

limitation on NCP. A negative correlation was found between the MLD and NCP_{vol} (Figure 10a, b) in both cruises. Due to the small sample size of selected stations and the latent variation in nutrients concentration among these stations, this correlation analysis did not necessarily mean that light played a key role in controlling NCP, but did imply a potential dependence of NCP on the light availability in the SCS. Higher NCP_{vol} mostly occurred at stations with shallower MLD (Figure 10) and a similar phenomenon was also reported by Cassar et al. (2011) in the subantarctic ocean south of Tasmania and by Hahm et al. (2014) in the Amundsen Sea in Antarctica. In addition, there was no relationship between MLD and NCP at the selected stations, since the correlations analysis was not statistically significant ($p > 0.05$) in both cruises. This result implied that there was no significant productivity below the mixed layer that was missed by underway sampling.

4 Conclusion

The distribution of $\Delta(O_2/Ar)$ and NCP on the northern slope of the SCS was strongly affected by nutrient availability, especially nitrogen, and was also subject to physical processes. In June 2015, we observed strong and rapid biological responses to the supply of nitrogen by shelf water injection. As a result, phytoplankton growth was enhanced and NCP was increase as well. In addition, dynamic processes such as vertical mixing caused by a cold eddy led to the errors of NCP estimates. The light availability may have also affected NCP, and higher NCP_{vol} were observed at stations with shallower MLDs in both cruises. The continuous measurements of O_2/Ar presented in this paper are of significance for studies of the highly dynamic carbon system in the SCS based on high-resolution NCP estimates.

Data Availability

All data presented in this manuscript are available on Weiyun.com (link: https://share.weiyun.com/ZtbQMNGl, password: p7rj36)

Author contribution

Guiling Zhang and Yu Han designed and set up the underway measurement system. Wenjing Zheng attended both cruises (in June 2015 and October 2014) in the South China Sea, and was mainly responsible for operating the underway measurement system during the cruises. Sumei Liu provided the nutrients data of both cruises. Chuan Qin attended the cruise in June 2015 and prepared the manuscript with contributions from all co-authors.

Acknowledgments

The authors wish to thank the crew of the *R/V* "Nanfeng" for the assistance with the collection of field samples and Professor Xiaoxia Sun for providing the ^{14}C-PP data. Professor Michael Bender and Bror Jonsson are acknowledged for constructive suggestions on the continuous O_2/Ar measurement system and the calculation of O_2/Ar-based NCP. This study was funded by the National Science Foundation of China through Grant Nos. 41776122, by the Ministry of Science and Technology of China through Grant Nos. 2014CB441502, by the Fundamental Research Funds for the Central Universities (No. 201562010), and by the Taishan Scholars Programme of Shandong Province (No. 201511014) and the Aoshan Talents Programme of the Qingdao National Laboratory for Marine Science and Technology (No. 2015ASTP-OS08).

Competing interests

The authors declare that they have no conflict of interest.

References:

Bi, Q., Du, J., Wu, Y., Zhou, J. and Zhang, J.: Particulate organic carbon export flux by $^{234}Th/^{238}U$ disequilibrium in the continental slope of the East China Sea, Acta Oceanol. Sin., 32(10), 67–73, doi:10.1007/s13131-013-0303-7, 2013.

Cai, P., Zhao, D., Wang, L., Huang, B. and Dai, M.: Role of particle stock and phytoplankton community structure in regulating particulate organic carbon export in a large marginal sea, J. Geophys. Res. Oceans, 120(3), 2063–2095, doi:10.1002/2014JC010432, 2015.

Cai, W.: Estuarine and Coastal Ocean Carbon Paradox: CO_2 Sinks or Sites of Terrestrial Carbon Incineration?, Ann. Rev. Mar. Sci., 3(1), 123–145, doi:10.1146/annurev-marine-120709-142723, 2011.

Cassar, N., Difiore, P. J., Barnett, B. A., Bender, M. L., Bowie, A. R., Tilbrook, B., Petrou, K., Westwood, K. J., Wright, S. W. and Lefevre, D.: The influence of iron and light on net community production in the Subantarctic and Polar Frontal Zones, Biogeosciences, 8(2), 227–237, doi:10.5194/bg-8-227-2011, 2011.

Cassar, N., Nevison, C. D. and Manizza, M.: Correcting oceanic O_2/Ar-net community production estimates for vertical mixing using N_2O observations, Geophys. Res. Lett., 41(24), 8961–8970, doi:10.1002/2014GL062040, 2014.

Chen, J., Zheng, L., Wiesner, M. G., Chen, R., Zheng, Y. and Wong, H.: Estimations of primary production and export production in the South China Sea based on sediment trap experiments, Chinese Sci. Bull., 43(7), 583–586, doi:10.1007/BF02883645, 1998.

Chen, W., Cai, P., Dai, M. and Wei, J.: $^{234}Th/^{238}U$ disequilibrium and particulate organic carbon export in the northern South China Sea, J. Oceanogr., 64(3), 417–428, doi:10.1007/s10872-008-0035-z, 2008.

Chen, Y. and Tang, D.: Eddy-feature phytoplankton bloom induced by a tropical cyclone in the South China Sea, Int. J. Remote Sens., 33(23), 7444–7457, doi:10.1080/01431161.2012.685976, 2012.

Chen, Z., Yang, C., Xu, D. and Xu, M.: Observed hydrographical features and circulation with influences of cyclonic-anticyclonic eddy-pair in the northern slope of the South China Sea during June 2015 (in Chinese), J. Mar. Sci., 34(4), 10–19, doi:10.3969/j.issn.1001-909X.2016.04.002,

https://doi.org/10.5194/os-2020-69
Preprint. Discussion started: 21 July 2020

Ocean Science Discussions
Open Access
EGU

2016.

Cheng, G., Sun, J., Zu, T., Chen, J. and Wang, D.: Analysis of water masses in the northern South China Sea in summer 2011 (in Chinese), J. Trop. Oceanogr., 33(3), 10–16, doi:10.3969/j.issn.1009-5470.2014.03.002, 2014.

Chou, W., Lee Chen, Y., Sheu, D., Shih, Y., Han, C., Cho, C., Tseng, C. and Yang, Y.: Estimated net community production during the summertime at the SEATS time-series study site, northern South China Sea: Implications for nitrogen fixation, Geophys. Res. Lett., 33(22), doi:10.1029/2005GL025365, 2006.

Clark, D. R., Rees, A. P. and Joint, I.: Ammonium regeneration and nitrification rates in the oligotrophic Atlantic Ocean: Implications for new production estimates, Limnol. Oceanogr., 53(1), 52–62, doi:10.4319/lo.2008.53.1.0052, 2008.

Craig, H. and Hayward, T.: Oxygen Supersaturation in the Ocean: Biological Versus Physical Contributions, Science, 235(4785), 199–202, doi:10.1126/science.235.4785.199, 1987.

Dugdale, R. C. and Goering, J. J.: Uptake of New and Regenerated Forms of Nitrogen in Primary Productivity, Limnol. Oceanogr., 12(2), 196–206, doi:10.4319/lo.1967.12.2.0196, 1967.

Eveleth, R., Cassar, N., Sherrell, R. M., Ducklow, H., Meredith, M. P., Venables, H. J., Lin, Y. and Li, Z.: Ice melt influence on summertime net community production along the Western Antarctic Peninsula, Deep Sea Res. Part II Top. Stud. Oceanogr., 139, 89–102, doi:10.1016/j.dsr2.2016.07.016, 2017.

Fan, L., Su, Y. and Li, F.: Analysis on water mases in the Northern South China Sea (in Chinese), Acta Oceanol. Sin., 10(2), 136–145, 1988.

Feng, S., Li, F. and Li, S.: An introduction to marine science (in Chinese), Higher Education Press, Beijing, China., 1999.

Guéguen, C. and Tortell, P. D.: High-resolution measurement of Southern Ocean CO_2 and O_2/Ar by membrane inlet mass spectrometry, Mar. Chem., 108(3–4), 184–194, doi:10.1016/j.marchem.2007.11.007, 2008.

Hahm, D., Rhee, T. S., Kim, H. C., Park, J., Kim, Y. N., Shin, H. C. and Lee, S.: Spatial and temporal variation of net community production and its regulating factors in the Amundsen Sea, Antarctica, J. Geophys. Res. Oceans, 119(5), 2815–2826, doi:10.1002/2013JC009762, 2014.

Hamme, R. C., Cassar, N., Lance, V. P., Vaillancourt, R. D., Bender, M. L., Strutton, P. G., Moore,

https://doi.org/10.5194/os-2020-69
Preprint. Discussion started: 21 July 2020

T. S., DeGrandpre, M. D., Sabine, C. L., Ho, D. T. and Hargreaves, B. R.: Dissolved O_2/Ar and other methods reveal rapid changes in productivity during a Lagrangian experiment in the Southern Ocean, J. Geophys. Res. Oceans, 117(C4), 92–99, doi:10.1029/2011JC007046, 2012.

Han, A., Dai, M., Gan, J., Kao, S., Zhao, X., Jan, S., Li, Q., Lin, H., Chen, C., Wang, L., Hu, J., Wang, L. and Gong, F.: Inter-shelf nutrient transport from the East China Sea as a major nutrient source supporting winter primary production on the northeast South China Sea shelf, Biogeosciences, 10(12), 8159–8170, doi:10.5194/bg-10-8159-2013, 2013.

He, X., Xu, D., Bai, Y., Pan, D., Chen, C. A., Chen, X. and Gong, F.: Eddy-entrained Pearl River plume into the oligotrophic basin of the South China Sea, Cont. Shelf Res., 124, 117–124, doi:10.1016/j.csr.2016.06.003, 2016.

Hu, J., Kawamura, H., Hong, H. and Qi, Y.: A Review on the currents in the South China Sea: Seasonal circulation, South China Sea warm current and Kuroshio intrusion, J. Oceanogr., 56(6), 607–624, doi:10.1023/A:1011117531252, 2000.

Huang, Y., Yang, B., Chen, B., Qiu, G., Wang, H. and Huang, B.: Net community production in the South China Sea Basin estimated from in situ O_2 measurements on an Argo profiling float, Deep Sea Res. Part I Oceanogr. Res. Pap., 131, 54–61, doi:10.1016/j.dsr.2017.11.002, 2018.

Izett, R. W., Manning, C. C., Hamme, R. C. and Tortell, P. D.: Refined Estimates of Net Community Production in the Subarctic Northeast Pacific Derived From ΔO_2/Ar Measurements With N_2O-Based Corrections for Vertical Mixing, Global Biogeochem. Cycles, 32(3), 326–350, doi:10.1002/2017GB005792, 2018.

Jiang, Z., Huang, C., Dai, M., Kao, S., Hydes, D. J., Chou, W. and Janf, S.: Short-term dynamics of oxygen and carbon in productive nearshore shallow seawater systems off Taiwan: Observations and modeling, Limnol. Oceanogr., 56(5), 1832–1849, doi:10.4319/lo.2011.56.5.1832, 2011.

Kaiser, J., Reuer, M. K., Barnett, B. and Bender, M. L.: Marine productivity estimates from continuous O_2/Ar ratio measurements by membrane inlet mass spectrometry, Geophys. Res. Lett., 32(19), 1–5, doi:10.1029/2005GL023459, 2005.

La Roche, J.: Ammonium regeneration: its contribution to phytoplankton nitrogen requirements in a eutrophic environment, Mar. Biol., 75(2–3), 231–240, doi:10.1007/BF00406007, 1983.

Lee Chen, Y.: Spatial and seasonal variations of nitrate-based new production and primary production in the South China Sea, Deep Sea Res. Part I Oceanogr. Res. Pap., 52(2), 319–340,

https://doi.org/10.5194/os-2020-69
Preprint. Discussion started: 21 July 2020

doi:10.1016/j.dsr.2004.11.001, 2005.

Lee Chen, Y. and Chen, H.: Seasonal dynamics of primary and new production in the northern South China Sea: The significance of river discharge and nutrient advection, Deep Sea Res. Part I Oceanogr. Res. Pap., 53(6), 971–986, doi:10.1016/j.dsr.2006.02.005, 2006.

Li, D., Zhou, M., Zhang, Z., Zhong, Y., Zhu, Y., Yang, C., Xu, M., Xu, D. and Hu, Z.: Intrusions of Kuroshio and Shelf Waters on Northern Slope of South China Sea in Summer 2015, J. Ocean Univ. China, 17(3), 477–486, doi:10.1007/s11802-018-3384-2, 2018.

Liu, M., Liu, X., Ma, A., Li, T. and Du, Z.: Spatio-temporal stability and abnormality of chlorophyll-a in the northern south china sea during 2002-2012 from MODIS images using wavelet analysis, Cont. Shelf Res., 75, 15–27, doi:10.1016/j.csr.2013.12.010, 2014.

Lockwood, D., Quay, P. D., Kavanaugh, M. T., Juranek, L. W. and Feely, R. A.: High-resolution estimates of net community production and air-sea CO_2 flux in the northeast Pacific, Global Biogeochem. Cycles, 26(4), doi:10.1029/2012GB004380, 2012.

Manning, C. C., Stanley, R. H. R., Nicholson, D. P., Smith, J. M., Timothy Pennington, J., Fewings, M. R., Squibb, M. E. and Chavez, F. P.: Impact of recently upwelled water on productivity investigated using in situ and incubation-based methods in Monterey Bay, J. Geophys. Res. Oceans, 122(3), 1901–1926, doi:10.1002/2016JC012306, 2017.

Millero, F. J. and Poisson, A.: International one-atmosphere equation of state of seawater, Deep Sea Res. Part A, Oceanogr. Res. Pap., 28(6), 625–629, doi:10.1016/0198-0149(81)90122-9, 1981.

Monterey, G. and Levitus, S.: Seasonal Variability of Mixed Layer Depth, NOAA Atlas NEDIS 14, U.S. Gov. Prinitng Off. D.C. [online] Available from: http://www.nodc.noaa.gov, 1997.

Nemcek, N., Ianson, D. and Tortell, P. D.: A high-resolution survey of DMS, CO_2, and O_2/Ar distributions in productive coastal waters, Global Biogeochem. Cycles, 22(2), doi:10.1029/2006GB002879, 2008.

Ning, X., Chai, F., Xue, H., Cai, Y., Liu, C. and Shi, J.: Physical-biological oceanographic coupling influencing phytoplankton and primary production in the South China Sea, J. Geophys. Res. Oceans, 109(10), doi:10.1029/2004JC002365, 2004.

Ning, X., Peng, X., Le, F., Hao, Q., Sun, J., Liu, C. and Cai, Y.: Nutrient limitation of phytoplankton in anticyclonic eddies of the northern South China Sea, Biogeosciences Discuss., 5(6), 4591–4619, doi:10.5194/bgd-5-4591-2008, 2008.

https://doi.org/10.5194/os-2020-69
Preprint. Discussion started: 21 July 2020

Ocean Science
Discussions
Open Access

Pan, X., Wong, G. T. F., Shiah, F. K. and Ho, T. Y.: Enhancement of biological productivity by internal waves: Observations in the summertime in the northern South China Sea, J. Oceanogr., 68(3), 427–437, doi:10.1007/s10872-012-0107-y, 2012.

Parsons, T. R., Maita, Y. and Lalli, C. M.: A Manual of Chemical & Biological Methods for Seawater Analysis, Pergamon Press, Oxford, UK., 1984.

Quay, P. D., Peacock, C., Bjrkman, K. and Karl, D. M.: Measuring primary production rates in the ocean: Enigmatic results between incubation and non-incubation methods at Station ALOHA, Global Biogeochem. Cycles, 24(3), doi:10.1029/2009GB003665, 2010.

Rehder, G. and Suess, E.: Methane and pCO_2 in the Kuroshio and the South China Sea during maximum summer surface temperatures, Mar. Chem., 75(1–2), 89–108, doi:10.1016/S0304-4203(01)00026-3, 2001.

Reuer, M. K., Barnett, B. A., Bender, M. L., Falkowski, P. G. and Hendricks, M. B.: New estimates of Southern Ocean biological production rates from O_2/Ar ratios and the triple isotope composition of O_2, Deep Sea Res. Part I Oceanogr. Res. Pap., 54(6), 951–974, doi:10.1016/j.dsr.2007.02.007, 2007.

Shadwick, E. H., Tilbrook, B., Cassar, N., Trull, T. W. and Rintoul, S. R.: Summertime physical and biological controls on O_2 and CO_2 in the Australian Sector of the Southern Ocean, J. Mar. Syst., 147, 21–28, doi:10.1016/j.jmarsys.2013.12.008, 2015.

Shi, X., Li, H., Han, X., Wang, L. and Zhu, C.: Influence of typical mesoscale oceanographical process on the distribution of nutrients and dissolved oxygen in the Northern part of South China Sea in summer (in Chinese), Acta Sci. Circumstantiae, 34(3), 695–703, doi:10.13671/j.hjkxxb.2014.0121, 2014.

Su, J. and Yuan, Y.: Coastal hydrology of China (in Chinese), China Ocean Press, Beijing, China., 2005.

Takahashi, T., Sutherland, S. C., Wanninkhof, R., Sweeney, C., Feely, R. A., Chipman, D. W., Hales, B., Friederich, G., Chavez, F., Sabine, C., Watson, A., Bakker, D. C. E., Schuster, U., Metzl, N., Yoshikawa-Inoue, H., Ishii, M., Midorikawa, T., Nojiri, Y., Körtzinger, A., Steinhoff, T., Hoppema, M., Olafsson, J., Arnarson, T. S., Tilbrook, B., Johannessen, T., Olsen, A., Bellerby, R., Wong, C. S., Delille, B., Bates, N. R. and de Baar, H. J. W.: Climatological mean and decadal change in surface ocean pCO_2, and net sea–air CO_2 flux over the global oceans, Deep Sea Res. Part

II Top. Stud. Oceanogr., 56(8–10), 554–577, doi:10.1016/j.dsr2.2008.12.009, 2009.

Tamminen, T.: Effects of ammonium effluents on planktonic primary production and decomposition in a coastal brackish water environment I. Nutrient balance of the water body and effluent tests, Netherlands J. Sea Res., 16(C), 455–464, doi:10.1016/0077-7579(82)90050-3, 1982.

Teeter, L., Hamme, R. C., Ianson, D. and Bianucci, L.: Accurate Estimation of Net Community Production From O_2/Ar Measurements, Global Biogeochem. Cycles, 32(8), 1163–1181, doi:10.1029/2017GB005874, 2018.

Tortell, P. D.: Dissolved gas measurements in oceanic waters made by membrane inlet mass spectrometry, Limnol. Oceanogr. Methods, 3(1), 24–37, doi:10.4319/lom.2005.3.24, 2005.

Tortell, P. D., Asher, E. C., Ducklow, H. W., Goldman, J. A. L., Dacey, J. W. H., Grzymski, J. J., Young, J. N., Kranz, S. A., Bernard, K. S. and Morel, F. M. M.: Metabolic balance of coastal Antarctic waters revealed by autonomous pCO_2 and ΔO_2/Ar measurements, Geophys. Res. Lett., 41(19), 6803–6810, doi:10.1002/2014GL061266, 2014.

Tortell, P. D., Merzouk, A., Ianson, D., Pawlowicz, R. and Yelland, D. R.: Influence of regional climate forcing on surface water pCO_2, ΔO_2/Ar and dimethylsulfide (DMS) along the southern British Columbia coast, Cont. Shelf Res., 47, 119–132, doi:10.1016/j.csr.2012.07.007, 2012.

Ulfsbo, A., Cassar, N., Korhonen, M., Van Heuven, S., Hoppema, M., Kattner, G. and Anderson, L. G.: Late summer net community production in the central Arctic Ocean using multiple approaches, Global Biogeochem. Cycles, 28(10), 1129–1148, doi:10.1002/2014GB004833, 2014.

Uu, D. V. and Brankart, J. M.: Seasonal variation of temperature and salinity fields and water masses in the Bien Dong (South China) Sea, Math. Comput. Model., 26(12), 97–113, doi:10.1016/S0895-7177(97)00243-4, 1997.

Wang, N., Lin, W., Cheng, B. and Huang, B.: Metabolic states of the Taiwan Strait and the northern South China Sea in summer 2012 (in Chinese), J. Trop. Oceanogr., 33(4), 61–68, doi:10.3969/j.issn.1009-5470.2014.04.008, 2014.

Wanninkhof, R.: Relationship between wind speed and gas exchange over the ocean, J. Geophys. Res. Oceans, 97(C5), 7373–7382, doi:10.1029/92JC00188, 1992.

Weiss, R. F.: The solubility of nitrogen, oxygen and argon in water and seawater, Deep Sea Res. Oceanogr. Abstr., 17(4), 721–735, doi:10.1016/0011-7471(70)90037-9, 1970.

Zhai, W., Dai, M. and Cai, W.: Coupling of surface pCO_2 and dissolved oxygen in the northern

South China Sea: Impacts of contrasting coastal processes, Biogeosciences, 6(11), 2589–2598, doi:10.5194/bg-6-2589-2009, 2009.

Zheng, W., Zhou, W., Cao, W., Wang, G., Deng, L., Xu, W., Xu, Z., Li, C. and Cai, J.: Characterization of particle size distribution in the South China Sea basin during summer 2016 (in Chinese), J. Trop. Oceanogr., 37(5), 74–85, doi:10.11978/2018017, 2018.

https://doi.org/10.5194/os-2020-69
Preprint. Discussion started: 21 July 2020

Figure Captions:

Figure 1. Cruise tracks of two cruises in the slope region of the Northern South China Sea in **(a)** October 2014, **(b)** June 2015 (red numbers indicating transects). The sea level height anomaly (SLA) and geostrophic current during observations in June 2015 (Chen et al., 2016) are shown in **(c)**.

Figure 2. Surface distributions of **(a)** temperature, **(b)** salinity, **(c)** chlorophyll-a (Chl a), and **(d)** $\Delta(O_2/Ar)$ in October 2014

Figure 3. Surface distributions of **(a)** temperature, **(b)** salinity, **(c)** chlorophyll-a (Chl a), **(d)** dissolved oxygen (DO), **(e)** pCO_2, and **(f)** $\Delta(O_2/Ar)$ in June 2015

Figure 4. Surface distribution of NCP among the northern slope of SCS during the cruise in **(a)** October 2014 and **(b)** June 2015.

Figure 5. Zonal variations in **(a)** temperature, salinity, **(b)** $\Delta(O_2/Ar)$, **(c)** Chl a, NCP and surface concentration of ammonia (NH_4^+) along Transect 5 in October 2014. The plots of $\Delta(O_2/Ar)$ and NCP are 10-point Savitzky-Golay smoothed to give a better view of their distribution.

Figure 6. Meridional variations in **(a)** temperature, salinity, **(b)** $\Delta(O_2/Ar)$, pCO_2, **(c)** Chl a, NCP and surface concentration of DIN along Transect 4 in June 2015. The plots of $\Delta(O_2/Ar)$, pCO_2 and NCP are 10-point Savitzky-Golay smoothed.

Figure 7. Principal Component Analysis (PCA) among variables for **(a)** October 2014 and **(b)** June 2015 (Bartlett's test of sphericity: $p < 0.01$)

Figure 8. **(a)** T-S diagram of surface DIN concentration in June 2015. The stations influenced by shelf water were in the red circle. Correlation analysis between surface DIN concentration and **(b)** NCP (at sampling stations) and **(c)** $\Delta(O_2/Ar)$. The stations (characterized with $S < 33$) influenced by shelf water presented surface DIN concentration ≥ 0.27 μM.

Figure 9. Correlation analysis between underway $\Delta(O_2/Ar)$, NCP and physical parameters (temperature and salinity) in October 2014 **(a, b, c and d)** and June 2015 **(e, f, g and h)**.

Figure 10. Relationship of volumetric NCP (NCP_{vol}) and mixed layer depth (MLD) in **(a)** October 2014 and **(b)** June 2015

https://doi.org/10.5194/os-2020-69
Preprint. Discussion started: 21 July 2020

Ocean Science
Discussions
Open Access
EGU

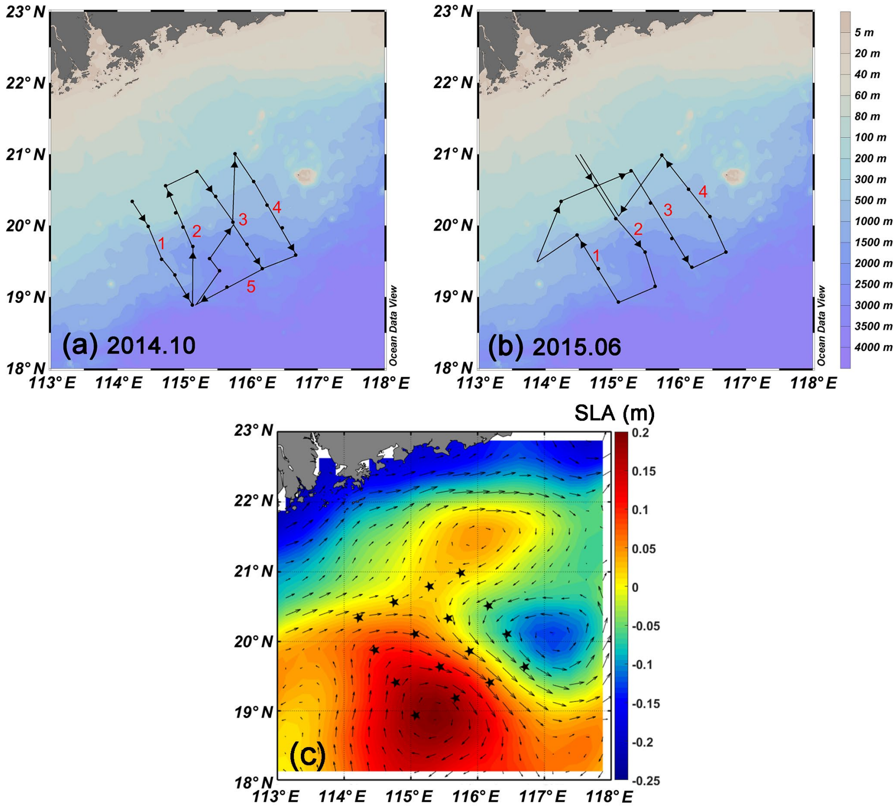

Figure 1. Cruise tracks of two cruises in the slope region of the Northern South China Sea in **(a)** October 2014, **(b)** June 2015 (red numbers indicating transects). The sea level height anomaly (SLA) and geostrophic current during observations in June 2015 (Chen et al., 2016) are shown in **(c)**.

https://doi.org/10.5194/os-2020-69
Preprint. Discussion started: 21 July 2020

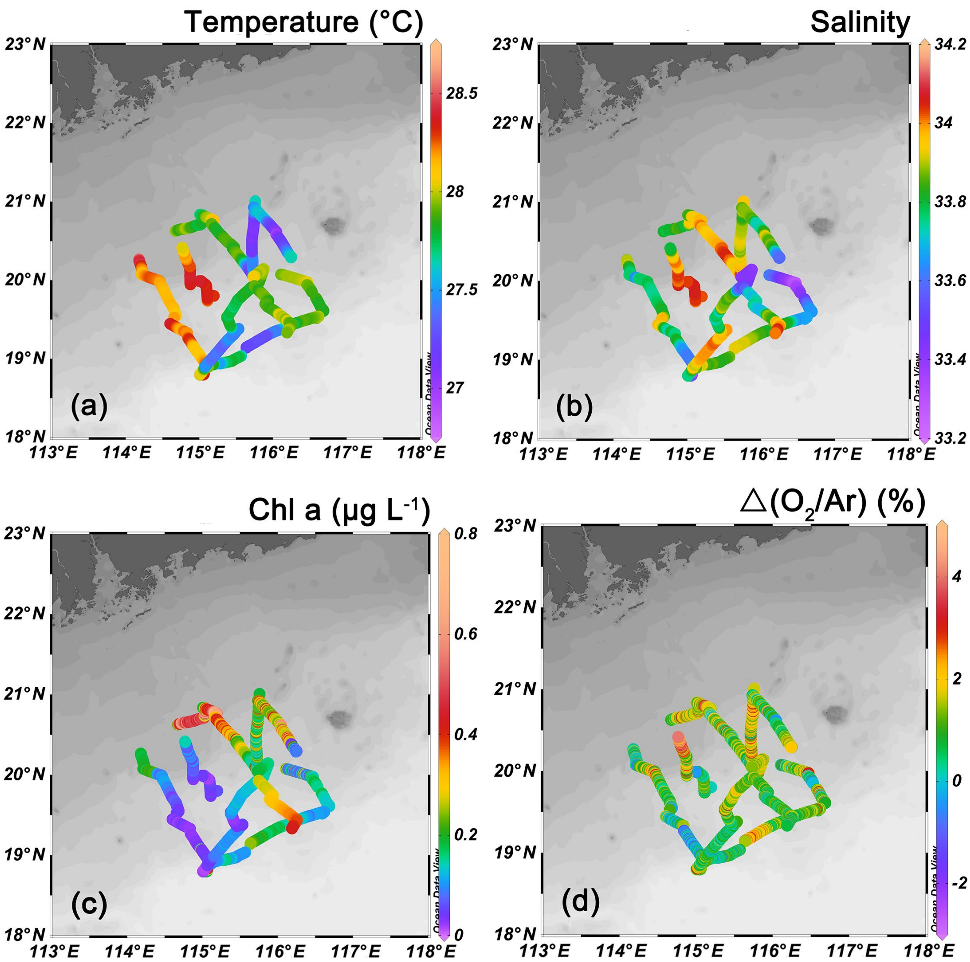

Figure 2. Surface distributions of (a) temperature, (b) salinity, (c) chlorophyll-a (Chl a), and (d) $\Delta(O_2/Ar)$ in October 2014

https://doi.org/10.5194/os-2020-69
Preprint. Discussion started: 21 July 2020

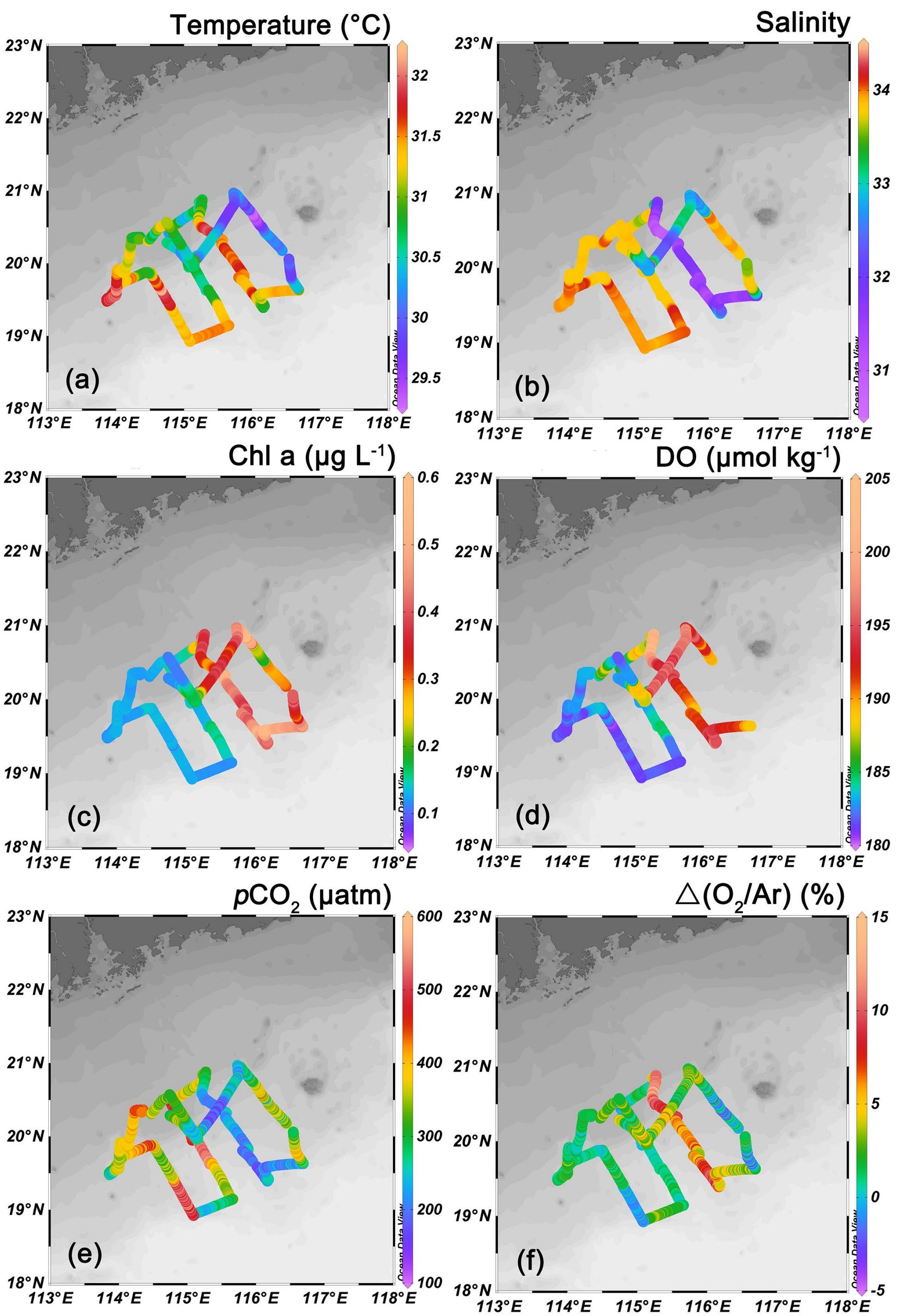

Figure 3. Surface distributions of **(a)** temperature, **(b)** salinity, **(c)** chlorophyll-a (Chl a), **(d)** dissolved oxygen (DO), **(e)** pCO$_2$, and **(f)** Δ(O$_2$/Ar) in June 2015

https://doi.org/10.5194/os-2020-69
Preprint. Discussion started: 21 July 2020

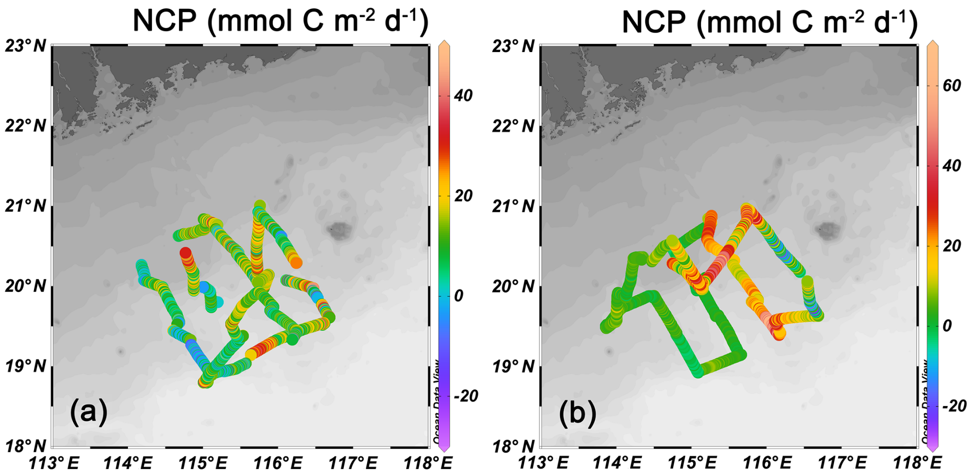

Figure 4. Surface distribution of NCP among the northern slope of SCS during the cruise in **(a)** October 2014 and **(b)** June 2015.

https://doi.org/10.5194/os-2020-69
Preprint. Discussion started: 21 July 2020

Ocean Science
Discussions
Open Access

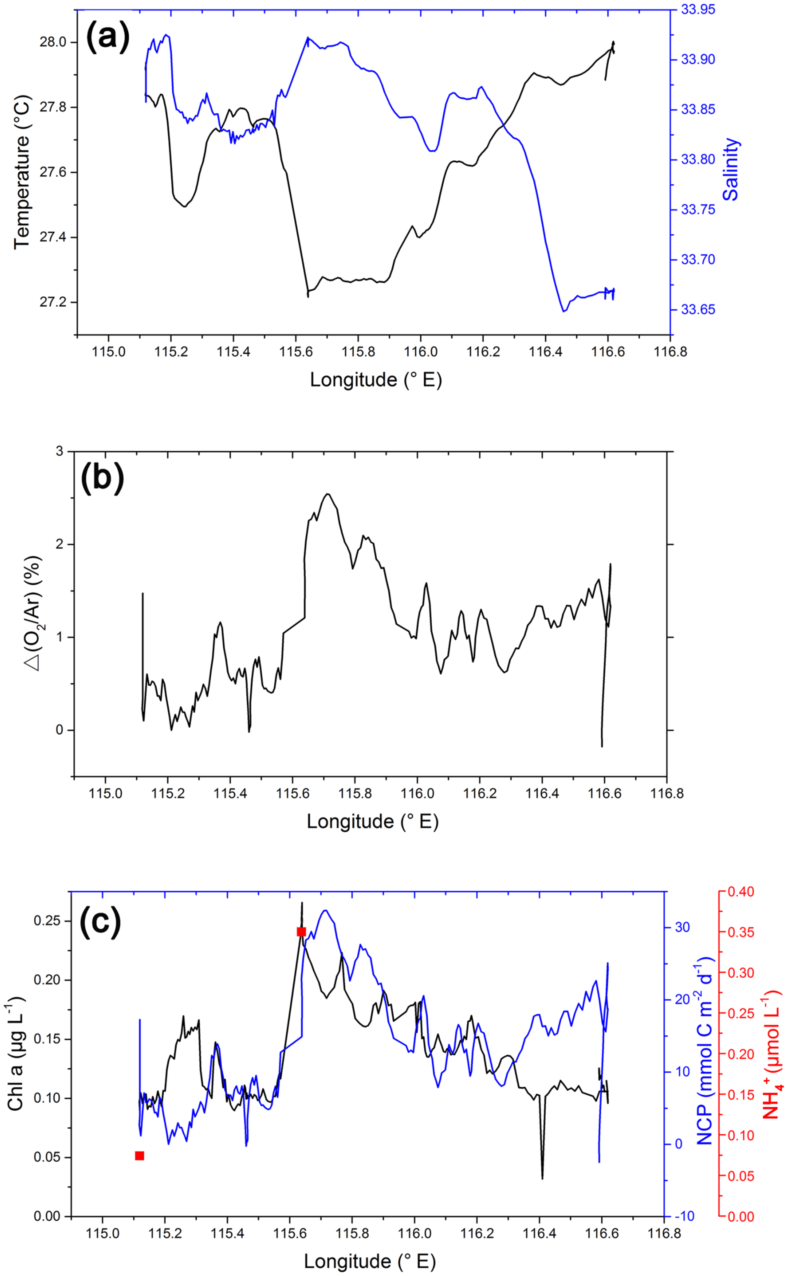

Figure 5. Zonal variations in **(a)** temperature, salinity, **(b)** $\Delta(O_2/Ar)$, **(c)** Chl a, NCP and surface concentration of ammonia (NH_4^+) along Transect 5 in October 2014. The plots of $\Delta(O_2/Ar)$ and NCP are 10-point Savitzky-Golay smoothed to give a better view of their distribution.

https://doi.org/10.5194/os-2020-69
Preprint. Discussion started: 21 July 2020

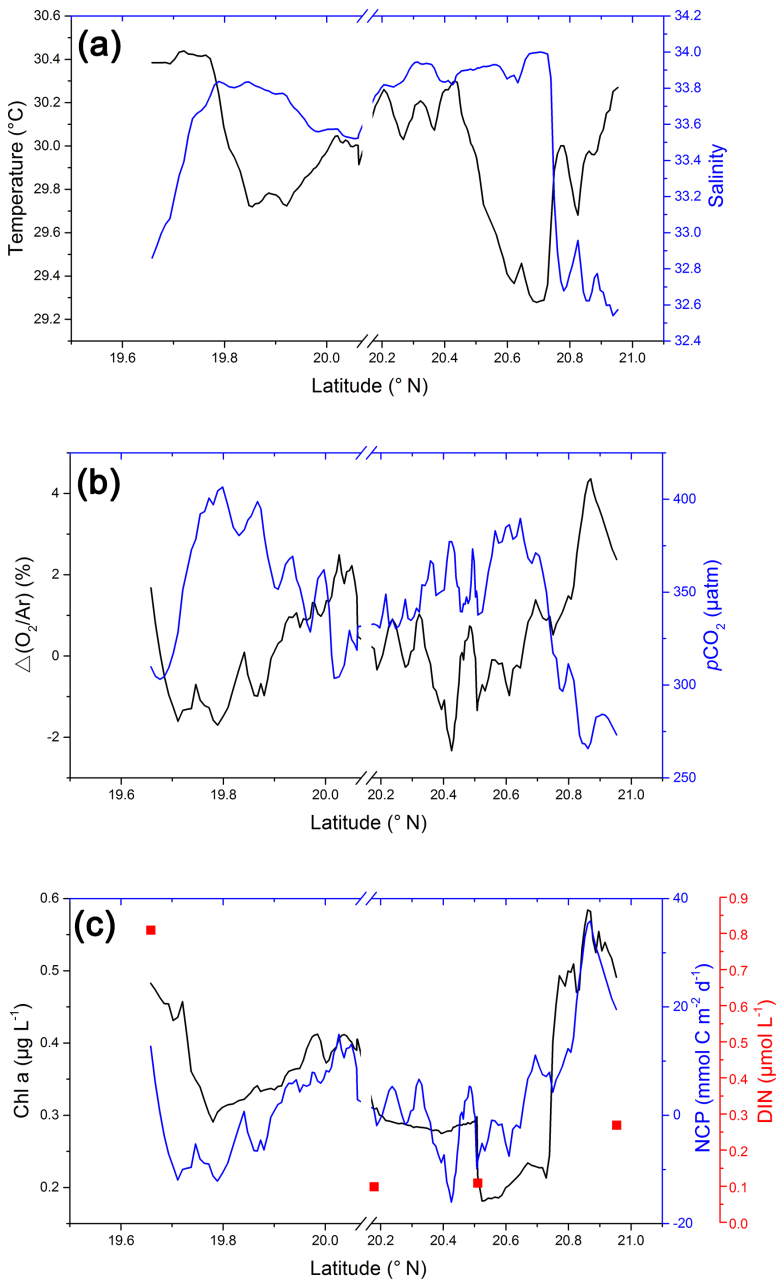

Figure 6. Meridional variations in **(a)** temperature, salinity, **(b)** $\Delta(O_2/Ar)$, pCO_2, **(c)** Chl a, NCP and surface concentration of DIN along Transect 4 in June 2015. The plots of $\Delta(O_2/Ar)$, pCO_2 and NCP are 10-point Savitzky-Golay smoothed.

https://doi.org/10.5194/os-2020-69
Preprint. Discussion started: 21 July 2020

Ocean Science
Discussions

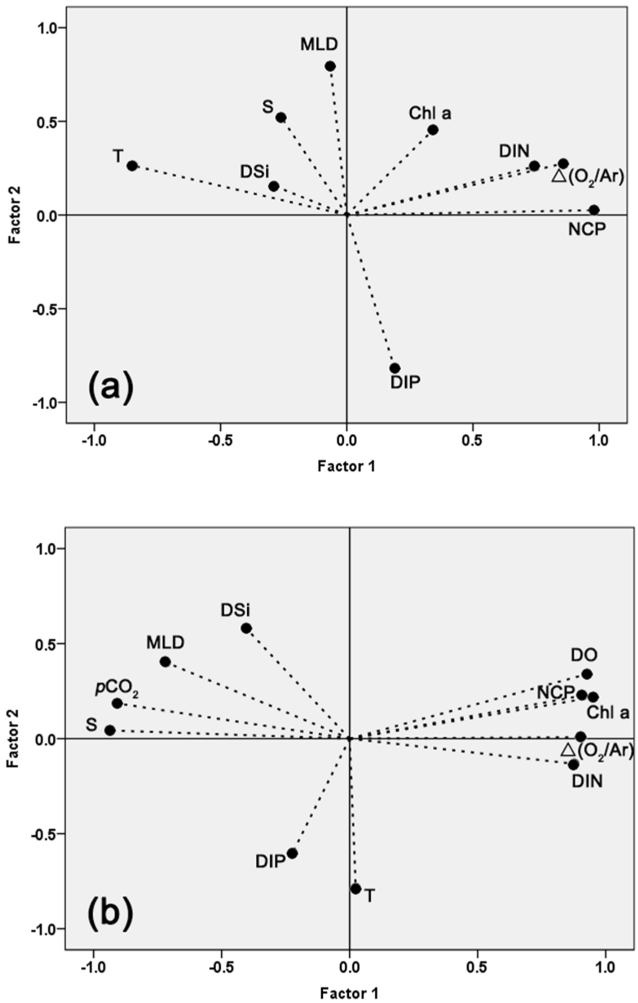

Figure 7. Principal Component Analysis (PCA) among variables for **(a)** October 2014 and **(b)** June 2015 (Bartlett's test of sphericity: $p < 0.01$)

https://doi.org/10.5194/os-2020-69
Preprint. Discussion started: 21 July 2020

Ocean Science
Discussions

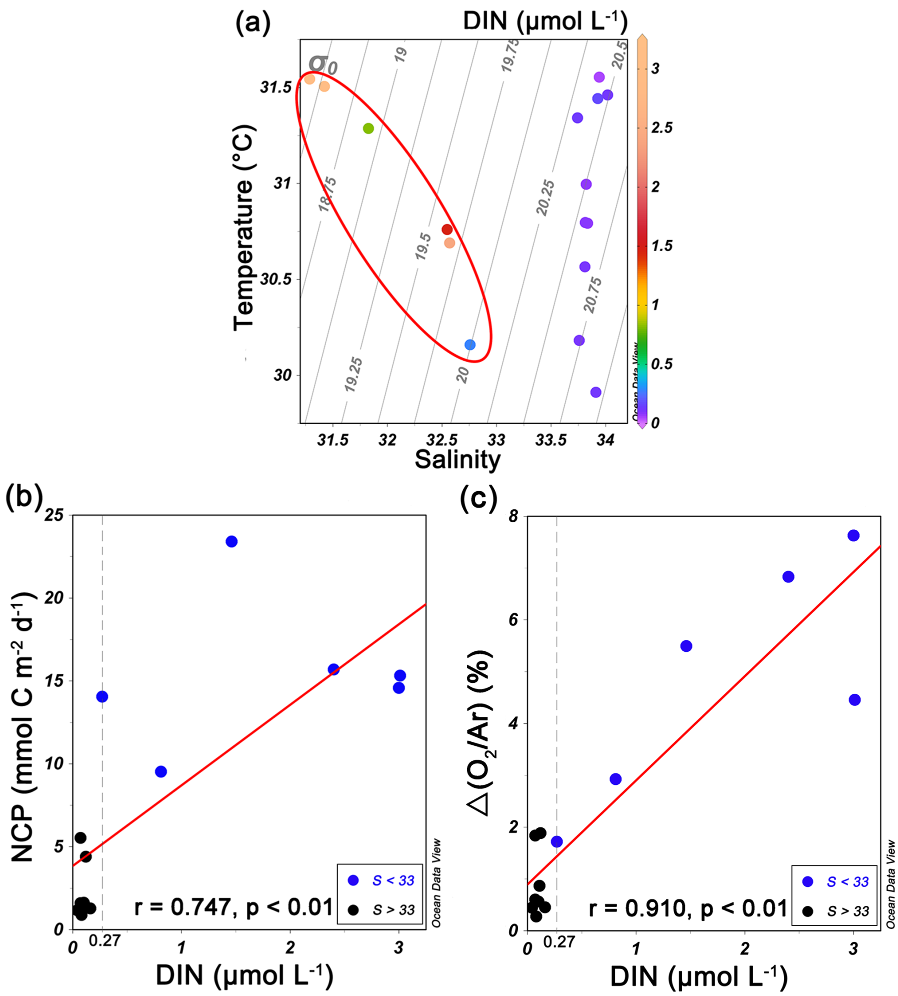

Figure 8. **(a)** T-S diagram of surface DIN concentration in June 2015. The stations influenced by shelf water were in the red circle. Correlation analysis between surface DIN concentration and **(b)** NCP (at sampling stations) and **(c)** $\Delta(O_2/Ar)$. The stations (characterized with $S < 33$) influenced by shelf water presented surface DIN concentration ≥ 0.27 μM.

https://doi.org/10.5194/os-2020-69
Preprint. Discussion started: 21 July 2020

Ocean Science Discussions
Open Access
EGU

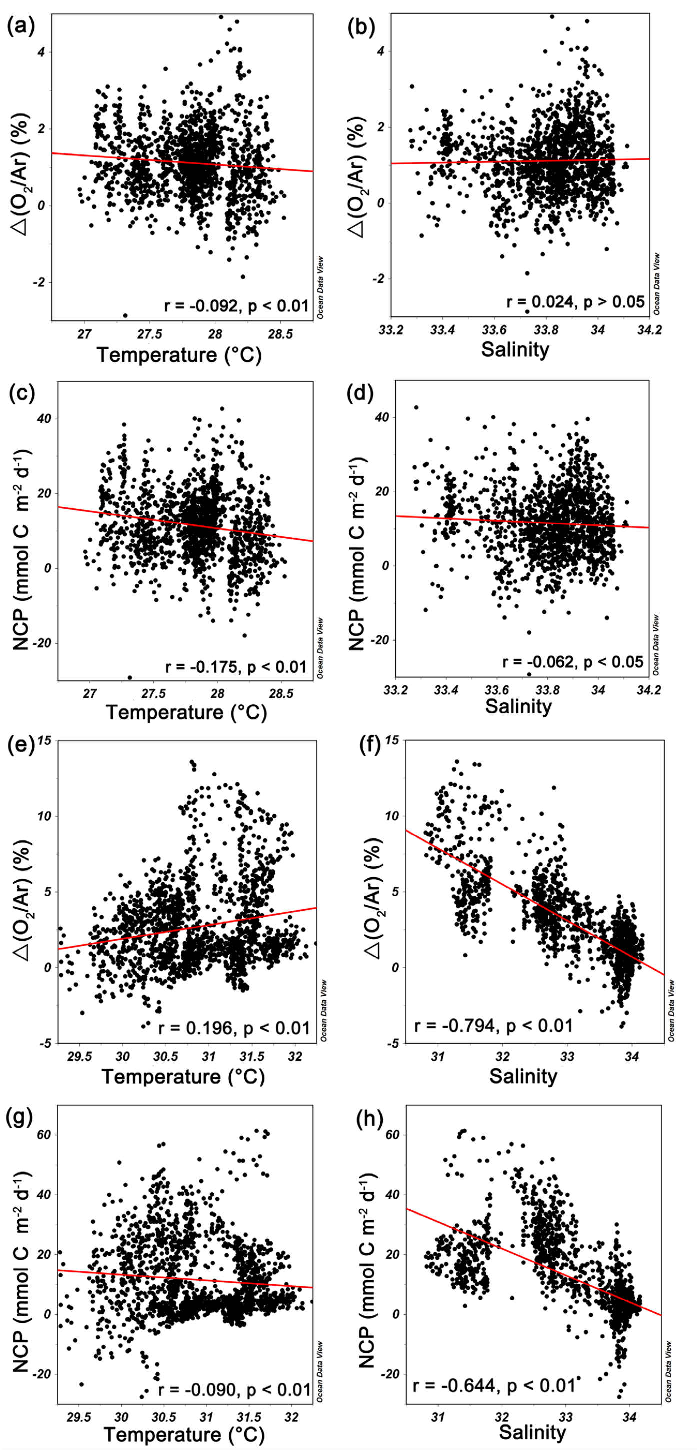

Figure 9. Correlation analysis between underway $\Delta(O_2/Ar)$, NCP and physical parameters (temperature and salinity) in October 2014 **(a, b, c and d)** and June 2015 **(e, f, g and h)**.

https://doi.org/10.5194/os-2020-69
Preprint. Discussion started: 21 July 2020

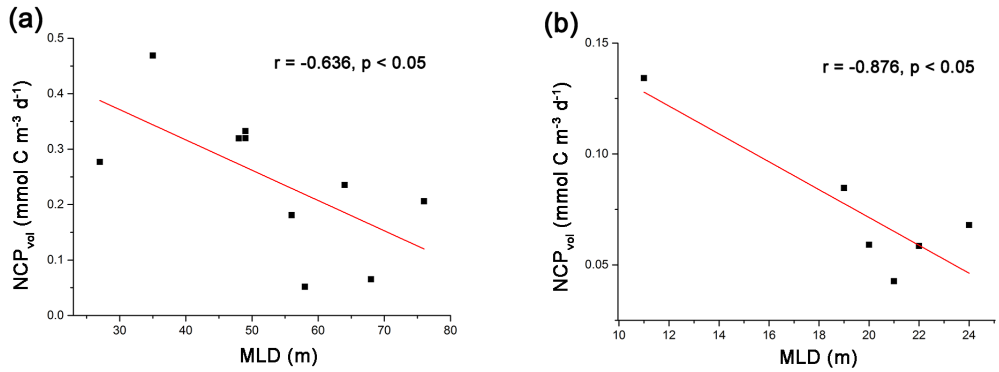

719

720 **Figure 10**. Relationship of volumetric NCP (NCP_{vol}) and mixed layer depth (MLD) in **(a)** October 2014 and **(b)** June 2015

721